JOINT EUROPEAN TORUS JET

JET–P(89)08

J.P. Coad, J.C.B. Simpson
and G.F. Neill

Combination of Ion Beam Techniques, AES and SIMS for the Analysis of Samples Exposed in the Plasma Boundary of the JET Tokamak

"This document contains JET information in a form not yet suitable for publication. The report has been prepared primarily for discussion and information within the JET Project and the Associations. It must not be quoted in publications or in Abstract Journals. External distribution requires approval from the Publications Officer, JET Joint Undertaking, Abingdon, Oxon, OX14 3EA, UK".

"Enquiries about Copyright and reproduction should be addressed to the Publications Officer, EFDA, Culham Science Centre, Abingdon, Oxon, OX14 3DB, UK."

The contents of this preprint and all other JET EFDA Preprints and Conference Papers are available to view online free at www.iop.org/Jet. This site has full search facilities and e-mail alert options. The diagrams contained within the PDFs on this site are hyperlinked from the year 1996 onwards.

Combination of Ion Beam Techniques, AES and SIMS for the Analysis of Samples Exposed in the Plasma Boundary of the JET Tokamak

J.P. Coad, J.C.B. Simpson
and G.F. Neill

JET-Joint Undertaking, Culham Science Centre, OX14 3DB, Abingdon, UK

Preprint of Paper to be submitted for publication in
Surface and Interface Analysis

COMBINATION OF ION BEAM TECHNIQUES, AES AND SIMS FOR THE ANALYSIS OF SAMPLES EXPOSED IN THE PLASMA BOUNDARY OF THE JET TOKAMAK

J P Coad, J C B Simpson and G F Neill
JET Joint Undertaking, Abingdon, Oxon OX14 3EA

ABSTRACT

A system combining ion beam and surface specific techniques for the analysis of probes exposed in the edge region of the plasma produced by the Joint European Torus (JET) is described. Among examples of the use of the system are the demonstration that 10 to 40% of the ionic charge flux in the boundary can be due to impurities, erosion and redeposition phenomena can be observed with small probes placed in the plasma boundary, and most of the oxygen observed on collector probes is an artefact resulting from exposure to air.

INTRODUCTION

This paper describes a specialised analysis system which combines ion beam analysis techniques (IBA) and the more surface specific techniques of Auger Emission Spectroscopy (AES) and X-Ray Photoelectron Spectroscopy (XPS) for the analysis of probes which are exposed in the boundary of the JET tokamak. The virtues (and limitations) of the combination of IBA and AES techniques (together with the use of SIMS in a separate system) will be expounded. However, first it is necessary to give some background details about the experiments.

If the energy released by the fusion of deuterium (^{2}H, or D) and tritium (^{3}H, or T) nuclei could be harnessed, it would provide an almost limitless source of energy. The most promising way of producing the right conditions for fusion is to create an intense plasma of ^{2}H and ^{3}H which is confined by magnetic fields. The most developed magnetic containment system is the tokamak, wherein the ions spiral round magnetic field lines within a toroidal vacuum vessel while staying within a closed flux surface. The Joint European Torus (JET) is the world's largest and most advanced tokamak experiment, and its objective is to demonstrate that the plasma parameters required for a commercial reactor can be achieved. The plasma parameters needed to produce an adequate fusion rate are

similar to those in the outer regions of the sun (specifically temperatures of 10-20 keV - approximately 100 to 200 million °C - densities of $\sim 2 \times 10^{20}$ m^{-3} and confinement times of 1-2 seconds([1],[2])). A further complication is that to reach these conditions the plasma may only contain very low levels of elements other than the ^{2}H and ^{3}H: any impurity elements dilute and cool the plasma, each effect being greater the heavier the impurity atom. However, the confinement of the plasma by the magnetic fields is not complete, and some interaction with the surroundings is inevitable. Firstly, it is necessary to have well-defined contact points to define the edge of the confined plasma (the so-called "last closed flux surface" (LCFS)), and these are called limiters. The limiters are subjected to a high flux of charged particles which travel round the torus under the action of the magnetic fields. The maximum power which can be applied to the plasma can be 40 MW in JET, and the majority of this may be conducted to the limiters. In order to spread this load over a large area, JET was fitted in 1987 with two continuous limiters, one located above and one below the outer midplane of the vessel (Figure 1). The particle flux decreases exponentially with distance away from the LCFS, but other components in the boundary region or "scrape-off layer" (SOL) may also receive a significant flux. Components may also be bombarded with particles which are not travelling parallel to field lines, particularly charge-exchange neutrals which after formation in the plasma may travel in any direction. These various interactions lead to considerable transport around the torus of impurity atoms that have been sputtered and then ionised. Most sputtering occurs at the leading edge of the limiters where the ion flux is greatest resulting in significant erosion, and net deposition may occur deeper into the SOL where impinging particle energies are generally lower ([3]).

Transport in the boundary region (SOL) is studied at JET using surface/collector probes which allow time-resolved information about impurity fluxes to be collected as a function of distance from the LCFS at two different points in the JET vacuum vessel (torus), using the Plasma Boundary Probe System (PBPS) which exposes probes at the top of the vessel, or the Fast Transfer System (FTS)/Surface Analysis Station (SAS) ([4],[5]). The FTS/SAS combination permits probes to be exposed near the outer midplane of the torus, returned to the diagnostic hall, and analysed in the SAS under ultra-high vacuum (UHV) (Figure 2): probes exposed using the PBPS can also be analysed in the SAS, but cannot be transferred under vacuum. This paper describes the analytical

techniques in some detail, and presents a number of results which demonstrate their application.

EXPERIMENTAL

(a) Collector probes and their exposure

The probes, shown schematically in the inset in Figure 2, consist of an outer cylindrical shield and an inner collector. The shield has a slit along the axial direction (which is as near normal to the LCFS as geometrical restraints on the FTS and PBPS permit) oriented so that the magnetic field lines are parallel to the sides of the slit: the flux of ions (which have a mean velocity parallel to the field lines) passing through the slit is thus maximised. Ions may be spiralling in either direction along the field-lines, although there is a small net surplus in one direction (the "ion drift direction"). Thus probes on the PBPS generally have two slits, one diametrically opposite the other, and differences in the fluxes measured through each slit are largely related to the relative distances along the intercepted field lines to the next object in the boundary region (eg. a limiter). However, probes exposed on the FTS normally have just one slit because the FTS enters the vessel close to the side of one of the eight RF antennas used to radiate power into the plasma as an additional method of plasma heating ([6]) (RF antennas can be seen between the limiters on the right-hand side of figure 1).

The collector within the shield may be a cylinder of high purity graphite which can be rotated during, or between, plasma pulses. However, since carbon is the principal impurity in JET (because the limiters are graphite) a special slotted collector is usually employed allowing ten rows of flat samples to be fitted which then approximate to a complete cylinder of that material: silicon, nickel or inconel have been used as samples. The rotation drive is programmed to move to a fresh area of sample at suitable times during a pulse (which typically lasts 20 secs), so that, for example, the periods of plasma current rise, steady maximum current, periods of additional heating (if any) and the current decay can be separately monitored. Alternatively if the total impurity level for a series of pulses is required, then the collector may be rotated between pulses so that a slit image is formed on a fresh area during each pulse. The position of the probe within the vessel is pre-set on the FTS and cannot be varied during a pulse: the probe location is chosen according to the predicted position of

the LCFS for that pulse, and subsequent measurements on the probe must be related to the actual distance from the LCFS at that time as determined from magnetic flux measurements. (The distance of the LCFS to the probes does vary somewhat during the pulse.)

The probe is held on a manipulator at the end of a train which is driven using linear induction motors to the torus along a 150 mm diameter UHV tube from the diagnostic hall, passing through the torus hall wall on the way (figure 2). Following exposure the train returns to the diagnostic hall, where the probe is replaced in a cassette which transports it to one of two analysis chambers (still under UHV).

(b) Analysis techniques

The SAS has two analysis chambers connected to the transport tube from the FTS. Each chamber has its own manipulator which reaches through the analysis chamber and grabs the collector mount, leaving the shield in the cassette so that the inner collector is presented to the analysis techniques. The manipulators can only hold the cylindrical collector with its axis horizontal, so there are restrictions on the sample orientations in the analysis chambers, furthermore as the manipulator passes through the centre of the analysis region it means that no part of a detector or excitation source assembly may be closer than 30 mm from the collector axis, or 14 mm from the analysis point on the collector surface (since the collector is 32 mm in diameter).

Chamber I is connected to an NEC 1.6 MV tandem accelerator, which can deliver $\sim$ 100 nA of protons or deuterons or helium 3 or helium 4 ions into an area of 1 or 2 mm in diameter for Ion Beam Analysis (IBA). The beam is incident normally for Rutherford Backscattering (RBS), Nuclear Reaction Analysis (NRA) or Particle Induced X-ray Emission (PIXE) analysis, and the collector can be moved sideways to allow glancing incidence (15°) and 30° detector angle for Elastic Recoil Detection (ERD) analysis of H and D (using 4 MeV $^4He^{++}$). Deuterium can also be analysed using the D(^{3}He, p)α reaction with 0.75 MeV $^3He^+$ ions, detecting both protons and alphas, or the D(d,p)T reaction which may be carried out simultaneously with C and O measurements using the $^{12}C(d,p_0)^{13}C$ and $^{16}O(d,p_1)^{17}O$ reactions at 0.9 MeV beam energy: the deuterium beam energy is currently limited to 1 MeV, but will be increased to 2 MeV when further shielding from energetic neutrons and gamma rays is completed. Carbon may also be detected by

$^{12}C(^{3}He,p_0)^{14}N$ NRA using 2.8 MeV $^{3}He^{++}$ and 150° detection angle. Carbon 13 is used as a marker for erosion probes (see section 3(c)) and can also be detected using the 0.9 MeV deuterium beam utilising the $^{13}C(d,\alpha_0)^{11}B$ reaction. Metals are analysed by RBS using a 2 MeV $^{4}He^{++}$ beam (which gives the total amount of the elements nickel + chromium + iron which are of particular interest to JET as the vacuum vessel is constructed from inconel), and simultaneously by PIXE for relative amounts of each element: the RBS is also useful for oxygen on carbon substrates. The IBA sensitivity realised at JET is about 10^{15} atoms cm^{-2} for all the elements listed above except ^{13}C for which the sensitivity is only about 10^{16} atoms cm^{-2}. However, background levels may limit the effective detection limits on the probes: for example, carbon and oxygen levels of a few $x10^{15}$ atoms cm^{-2} are normally found on metal substrates, though experiments using ion guns to clean up probes prior to exposure are in hand to try to improve this, and some metals (particularly iron) are found on the machined graphite collectors.

Chamber II contains a hemi-spherical electron analyser with electron and X-ray sources for Auger and X-ray photoelectron spectroscopies (respectively). The electron gun can be focused to better than 1 μm spot size and rastered for electron imaging of the sample surface, but for AES the beam is somewhat defocused to operate at 5 keV and ∿ 20 nA: the analyser is run in the n(E) mode. An ion gun is fitted to the chamber to permit depth profiling by sequential argon ion sputtering and Auger analysis. The gun can be focused to ∿ 200 μm spot size, but with the restricted geometry imposed by the collector probes and manipulator it is too difficult to align the ion and electron guns so that the beam spots coincide to use this mode, and the ion beam is rastered over an area of ∿ 3x3mm. The XPS part of the system has not been used in this work.

SIMS analysis was carried out in a separate CAMECA 3F ion analyser, using 15 keV O_2^+ ions at a beam current of 1 μA. The primary beam raster area was 175 to 350 μm square whilst (positive) secondary ions were extracted from areas either 60 or 10 μm in diameter.

RESULTS

(a) Measurements of impurity fluxes in the SOL

The carbon, oxygen and metal impurity concentrations measured near the centre of the plasma are typically 3, 0.5 and 0.01% of the average electron density over the confined volume of the plasma (equivalent to the average density of ionic charges since the plasma is neutral). However, impurity concentrations in the SOL are likely to be higher, since the impurities must emanate from this region, and careful studies of the impurity profiles may elucidate release mechanisms. In order to obtain impurity concentrations, the impurity (C, O, Metal) fluences are first measured as a function of time by the use of collector probes. (It is assumed in this paper that the impurities are collected with 100% efficiency, ie. every impurity atom entering the slit sticks to the probe surface, though experiments are in hand to investigate this assumption in detail.) From the rotation sequence of the probe the measured fluences are then expressed as fluxes of atoms cm^{-2} sec^{-1} at various times in the discharge, and as functions of distances from the LCFS. The amounts of deuterium (and sometimes hydrogen) incorporated from the plasma is also measured but this is generally not the flux of D (or H) at the probes, because the amounts that can be retained are the (smaller) amounts that can be implanted into the substrate or that can be co-deposited with the carbon (up to 0.4 times the amount of C ([7])). The total number of positive charges incident at a similar point in the boundary (the "ion saturation current") can be measured using a negatively biased electrode: such electrodes are called Langmuir probes ([8]) and many are present in the boundary region of JET, including a set of three on another manipulator on the FTS measuring parallel to the slit on the collector probe. Mean ion temperatures and densities can also be derived from the Langmuir probe data ([8,9]), but it is the ion saturation current which allows the impurity concentrations to be converted to percentages of the local ion fluxes.

Figure 3 shows the carbon, deuterium and nickel fluxes measured at a point which was exposed 10 mm behind the protection tiles for the RF antenna. At closest approach of the plasma (6 to 16 secs) this was 22 mm from the LCFS for the JET pulses 13840 and 13841. Since these 3.5 MA flat-top pulses were identical except for the amount of additional RF heating (which is too low to have a significant effect on the boundary), data for the two pulses are overlaid. For each measured level, the horizontal length of the bar indicates over which time the data was collected. (Data collected from 8-11 secs in shot 13841 are missing due to a dead space in the movement of the analysis chamber manipulator). The C and D levels were determined by NRA and the Ni by PIXE. Figure 4 shows the "ion saturation current" (I_{sat}) at three distances behind the

leading edge of the RF antenna tiles at the midplane, 5 mm (1), 10 mm (3) and 23 mm (4), for pulse 13841 (results from 13840 are very similar). The variation in I_{sat} with time into the pulse is similar to that of the carbon, showing that the carbon is a roughly constant fraction of the total ion flux during the pulse. At 13 secs into the discharge, when the LCFS was in contact with the RF antenna tiles at the midplane, the carbon flux collected was 3.6×10^{16} atoms cm^{-2} sec^{-1} compared with an I_{sat} of 3.4×10^{17} charge units cm^{-2} sec^{-1}, which would mean 10% of the ion flux was carbon if the carbon ions collected were singly ionised. However, charge states up to 4+ are quite probable within the boundary region, and if all the carbon was incident as C^{4+} this would account for 44% of the so-called "I_{sat}", which would mean a large error in the underlying assumption made when interpreting Langmuir probe data that the current is from singly charged deuterium ions.

Whatever the charge state of the carbon, the ion current still implies many more deuterium ions reach the collector than carbon ions. However, figure 3 shows that the deuterium level observed is $\sim$ 0.4 times the amount of carbon, ie. agrees with the saturation level for deuterium in a carbon film (7). Thus, the amount of deuterium (or more generally hydrogen isotopes) collected on such probes does not reflect the incident flux of deuterium, but rather is proportional to the flux of carbon, provided that there are not significant amounts of implantation into the substrate and the deuterium flux is larger than the amount required to saturate the layer. An example of the use of this information is in the next section. The nickel level observed at 13 secs represents $\sim$ 0.03% of the ion flux in the boundary, which is comparable to the level in the plasma, and suggests that the nickel collected has come from the plasma, rather than from a local source. The general shape of figures 3 and 4 does not reflect the plasma current, which was constant at 3.5 MA from 4 to 15 secs. The precise position of the LCFS with respect to the various probes is critical, since the exponent of the current fall-off in the SOL is just 8.5 mm, but even allowing for this there are still variations in the fluxes which are due to the detailed power balance and loading of components in the boundary region.

(b) Demonstration of Net Erosion Near the LCFS

Examination of limiter tiles after $\sim$ 2800 pulses over an 11 month operational period (1986) showed a net erosion at the leading edge of the tiles (plasma

contact area) of ∿ 200 μm and deposition on the flanks of the tile (20-40 mm from the LCFS) of up to 100 μm. In 1986 the FTS was used to insert carbon probes (non-rotating) close to the LCFS (nearest point 10 mm from the LCFS) for just two 5 MA pulses ([10],[11]). The probes were implanted with a dose of 3 x 10^{17} atoms cm^{-2} of carbon 13 to a mean range of 80 nm, and after exposure the probes were examined with SIMS as well as IBA. IBA showed large amounts of deuterium (and by inference large deposits (up to 0.2 μm) of carbon) with a low level of incorporated nickel over all the probe, though decreasing with a rather long exponential folding length (∿ 55 mm) away from the LCFS. SIMS confirmed that more than 30 mm from the LCFS there was a thick film of carbon (+ deuterium) overlaying the surface, as determined by the ^{13}C marker, however close to the end of the probe the marker was absent, indicating that there must have been erosion as well as the observed deposition. In the present experiments ^{13}C was implanted into the collector to two different depths (80 and 300 nm) by using 40 and 150 keV implantation energies, respectively, with a dose of 3 x 10^{17} ions cm^{-2} at each energy. Time resolution was achieved by rotating the collector within the shield during the pulse, however a wide (15 mm) slit was used in order to prevent erosion from the shield causing deposition on the collector, so only a simple separation between the current rise, flat top and current rampdown phases of the discharge was possible.

Figure 5 shows NRA spectra recorded using a deuteron beam from various points along the region of the probe that was exposed to the 10 secs flat top of a 3 MA discharge (17928): the distance during exposure of each analysis point from the LCFS (Z) is indicated. The area at the largest distance (Z=89) was actually beyond the end of the slit, so can be taken as an unexposed (reference) region. The ^{13}C is clearly detected, but the deeper implant is not resolved from the side of the peak from the shallower implant (the higher the channel number, or particle energy, the nearer the surface): deuterium is not detectable in this area. Closer to the plasma (Z=71 and Z=53) deuterium is shown to increase, and the ^{13}C broadens and shifts, suggesting a D-containing layer of rather variable thickness overlying the surface. At a point exposed 25 mm from the plasma the amount of deuterium is considerably greater, but the ^{13}C is no longer obvious, possibly because it is too far from the surface to be detectable. At 17 mm from the LCFS no deuterium remains, and there is a significant peak from a metal (identified by PIXE as mostly Ni): reduction in the deuterium occurs sharply at ∿ 25 mm from the LCFS (figure 6). Although there appears as if there might be a little ^{13}C present at Z=17mm at close to its original depth, this is illusory:

careful measurements with long counting times detected no ^{13}C within 30 mm of the LCFS.

The same region of the probe was examined in a separate vacuum system by SIMS. Figure 7 shows the relative signals from carbon 12 (using mass 24) carbon 13, oxygen, deuterium and nickel from an area exposed $\sim$ 70 mm from the LCFS as a function of bombardment time (ie. depth into the surface). In this region the ^{13}C gives a clear peak below the deposited film (which is defined by the deuterium). The peak in ^{13}C results in a corresponding dip in the mass 24 level of about 10%, which suggests that the ^{13}C is present at 10% of the ^{12}C in this region. Note that the two implantation peaks expected theoretically are not resolved, in just the same way as observed in the shadowed region by IBA (figure 5). This suggests that the sharp implantation profiles were not realised on this graphite probe with a fairly rough, porous surface: sharper profiles have been obtained in the past on polished, oriented graphite. The natural abundance of ^{13}C in carbon is 1%, so as the film overlaying the implants thickens nearer the plasma-facing end of the probe, the SIMS peak from ^{13}C broadens and is less intense due to variations in film thickness and sputter induced surface roughening until it cannot be distinguished from the background. As a result ^{13}C can only be seen by SIMS in the same areas as it can be seen by IBA.

Following exposure in the torus, samples in general show remarkably little oxygen incorporation in the films, despite the fact that the oxygen impurity level in the plasma core may be about 10% of that of carbon. On the limiter probe, for example, the detection level of oxygen by IBA is $< 10^{16}$ atoms cm^{-2}, which at some points is more than two orders of magnitude less than the amount of carbon present, yet oxygen was not observed. Furthermore, Auger analysis was unable to detect oxygen on the surface, so that in the outer 1 nm the oxygen level must also be much less than 1%. However, after exposure to air for 1 hour oxygen could be clearly seen by NRA in the region where a film had been deposited (but not elsewhere), as shown in figure 8: the broad feature in figure 8 due to oxygen implies the oxygen was not absorbed on the surface, but was present at a low concentration throughout the film. The oxygen uptake is approximately 5% of the amount of carbon deposit, as shown in figure 6, whilst AES gives a similar oxygen concentration at the very surface. This is precisely the result reported in an earlier publication ([12]) for a film deposited in JET

on a silicon substrate, however that sample had been exposed to air prior to analysis since the FTS was not fully operational.

(c) Metallic Impurity Levels During RF Heating

Early in the 1987/8 JET operational campaign metallic impurity levels were observed to rise after extended use of RF heating (though not to a level at which they made a significant contribution to the radiated power). In order to check that the principal contribution to this impurity level was nickel from the Faraday screens of the antennae, a series of 10 similar 3 MA pulses was performed, with varying levels of additional RF and neutral beam heating. A 10-sided silicon collector probe was exposed on the FTS during this series, with each side being exposed to one complete discharge. Nickel was observed to be the principal metallic impurity by PIXE, and the amounts of nickel as a function of the RF heating power are plotted in figure 9. A closely linear relationship between nickel level and RF power can be seen, with two exceptions. For shot 13904 the dipole configuration was used instead of the monopole configuration, and this was known to produce less impurity influx (but appeared to couple less efficiently to the plasma). 13908 also produced less nickel per MJ than the norm, but the reason for this is unknown. It is clear from figure 9 that the power applied using the other method of additional heating at JET, neutral beam heating wherein beams of high energy deuterium atoms are fired into the plasma, (the number of megawatts given in brackets) has no relationship to the metal impurity level for the plasma. The central nickel impurity level for the plasma also exhibited a linear relationship with applied RF power. More recently, covering the screens with a layer of carbon by in-situ carbonisation (7) and a greater use of the dipole configuration has prevented significant nickel concentrations in the plasma during RF heating programmes.

DISCUSSION

Probes exposed in the boundary of the JET tokamak require the analysis of thin (< 1 μm) films which (until now) have been predominantly carbon with incorporated deuterium, hydrogen, oxygen and metals such as nickel, chromium and iron. These elements can all be analysed using ion beam techniques with sensitivities generally of the order of 10^{15} atoms cm^{-2}, and some information on the distribution with depth is also obtained non-destructively. If the elements are contained within a very thin layer (∿ a few nm), then sensitivity for C, O

and the metals is better by Auger Spectroscopy, but this may not be realised if there is a significant background for the element. For example, figure 10 shows that similar carbon distributions along a probe can be obtained by each technique, but AES has not been able to extend the profile further from the LCFS than IBA due to the inherent background, and for films > 1 nm thick the depth profiling necessary to derive the amount of C is time-consuming and destroys the information. However, if the probes could be cleaned (eg. by ion bombardment) and remained clean during the transport to and from the torus it might be possible to utilise the additional sensitivity of AES (and non-destructively for films < 1 nm thick): work is proceeding in this area. Another virtue of AES which has not been discussed in this paper is its much greater spatial resolution ($\sim$ 1 μm diameter, compared with $\sim$ 1 mm). Good spatial resolution has been essential in the analysis of other tokamak-related problems, for example droplet formation on the walls of the vacuum vessel.

The ability to exposure and analyse boundary probes in the same vacuum system has had a direct influence on the interpretation of oxygen impurity flux measurements. The FTS/SAS has shown that although oxygen is a significant plasma impurity, very little is collected in the SOL. However, on exposure to air oxygen is absorbed throughout the carbon-based deposits formed in the plasma boundary, to about 5% of the amount of carbon. It is thus incorrect to draw the apparent conclusion from air-exposed samples that the oxygen was an impurity collected in the SOL. The absence of a surface peak suggests the oxygen ingress is not due to a diffusion process, but that all the film is easily accessible from the gas phase, eg. may be porous, and that the oxygen is attracted to specific sites in the film structure. Reactivity of the surface films to the gas phase is also consistent with the observation that deuterium is released from surfaces within the torus on exposure to air at a mean value of around 10^{16} atoms cm^{-2} ([13]).

The comparison of collected impurities with Langmuir probe data provides a note of caution for interpretation of the latter data. The size of the correction to ion flux due to the impurities depends critically on the ionisation state of the impurities, which neither technique measures and at present can only be estimated. Probes appear to have demonstrated that erosion occurs near the plasma boundary, though from the IBA and SIMS results one cannot completely rule out the possibility that there is a very thick carbon film (through which the ^{13}C is not detectable) and the deuterium is lost by heating. However to reduce

the deuterium content by about 3 orders of magnitude requires a temperature of ∿ 1750°C ([14]) which would be visible (albeit by multiple reflection) in the torus viewing camera, and furthermore erosion of the shield was apparent visually. Experiments using a better system of determining the extent of erosion will be attempted in the next operating campaign, since the rate of erosion of components near the LCFS in high flux situations is critical to the design of future fusion devices which will duplicate the surface loadings required for a power generating reactor.

Fresh analytical problems will be presented in 1989 when beryllium is used as the first-wall material in JET. Be can be observed with NRA and AES (although in the latter case the peaks are at too low energy for high sensitivity and can be distorted by chemical effects). XPS may prove a useful adjunct for the IBA techniques in this case, since an important factor concerning the use of Be is its efficiency for gettering oxygen, especially when carbon is also present: detailed examinations of the Be peak in XPS may be very useful in elucidating this matter. Further into the future, analysis of tritium and helium will be important, both of which can be monitored by IBA.

CONCLUSIONS

Studies of the boundary region of the JET plasma with collector probes required the use of a combination of surface analytical techniques. Ion beam techniques provide the basic information, with NRA using a deuterium ion beam being particularly useful, however AES and SIMS have also had useful roles to play.

It has proved essential to have analytical techniques connected to the torus by a high vacuum delivery system since air exposure alters the analysis of the deposits on the collector probes. In particular, oxygen levels change drastically and in a very misleading manner when carbon-based films deposited in the plasma boundary are exposed to air.

The examples of plasma boundary investigation cited show that nickel impurity levels increase with RF heating power, Langmuir probe measurements in the boundary may be affected by the high impurity concentrations observed, and significant erosion of components in the boundary occurs close to the edge of the plasma.

The ion beam techniques will be useful for beryllium, tritium and helium analysis at JET in the future, but XPS is expected to be important also for beryllium analysis.

ACKNOWLEDGEMENT

Supplementary ion beam analysis has been carried out at the Max-Planck Institut für Plasmaphysik (IPP), Garching-bei-München and at the Manne Siegbahn Institute of Physics, Stockholm (MSI). SIMS analysis has been conducted by Loughborough Consultants and Surface Analysis Technology. The authors are idebted to J Partridge (Culham Laboratory), H Bergsaker (MSI), S Burch (Sussex University) and J Ehrenberg, C Nicholson and J Vince (JET) for assistance with analysis with, and operation of, the FTS/SAS.

REFERENCES

[1] P H Rebut and P P Lallia, 7th International Conference on Plasma Physics, Kiev, USSR, April 1987.

[2] P H Rebut and B E Keen, Fusion Technology 11 (1987) 13.

[3] G M McCracken et al, J Nuclear Materials 145-147 (1987) 621.

[4] R Charles et al, Proc 14th Symposium on Fusion Technology (Avignon, France 1986), pp1499-1504.

[5] C J Hancock et al, Proc 15th Symposium on Fusion Technology (Utrecht, Netherlands, 1988).

[6] A Kaye, J Jacquinot et al, Fusion Technology 11 (1987) 203.

[7] J Winter, J Nuclear Materials 145-147 (1987) 131

[8] S K Erents et al, Nuclear Fusion 26 (1986) 1591.

[9] S K Erents et al, Nuclear Fusion 28 (1988) 1209.

[10] J P Coad et al, 14th European Conference on Controlled Fusion and Plasma Physics, Madrid, June 1987.

[11] R Behrisch et al, J Nuclear Materials 163-165 (1989).

[12] H Bergsaker et al, 14th European Conference on Controlled Fusion and Plasma Physics, Madrid, June 1987.

[13] J P Coad et al, J Nuclear Materials 163-165 (1988).

[14] V Philipps et al, J Nuclear Materials 145-147 (1987) 292.

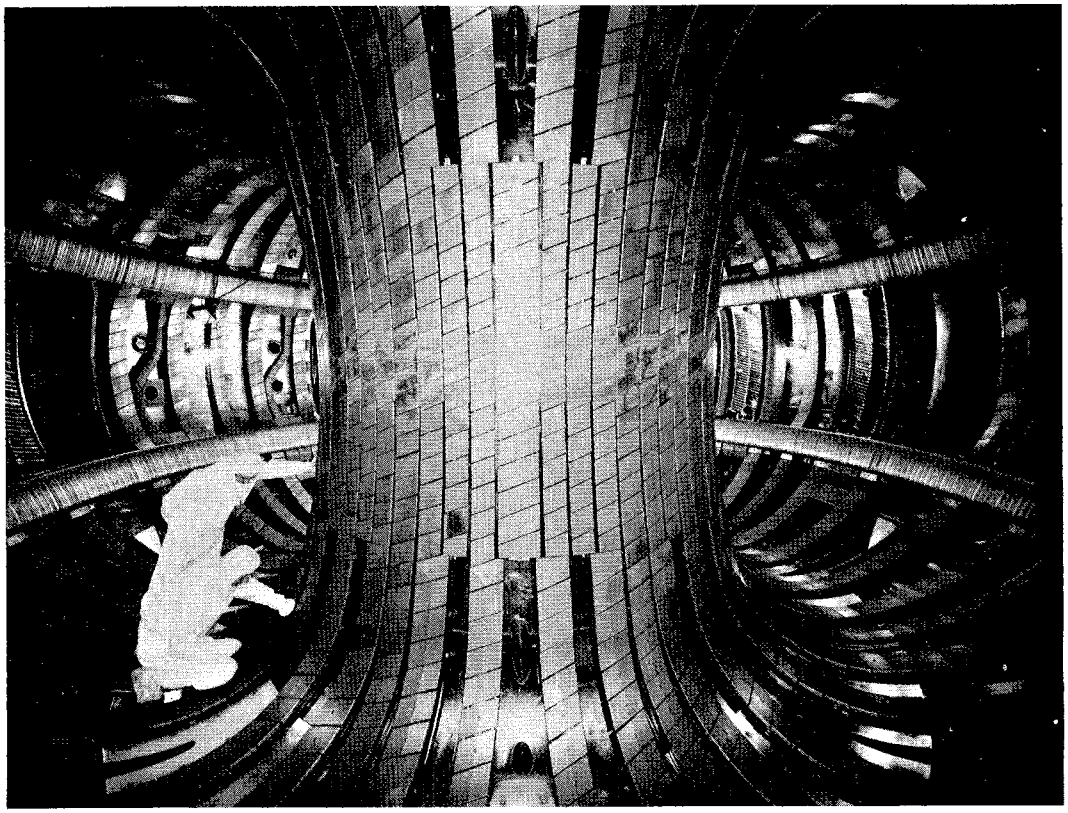

Fig. 1 View of the inside of the JET torus, as configured from mid-1987. The two belt limiters can be seen around the outer wall of the vessel.

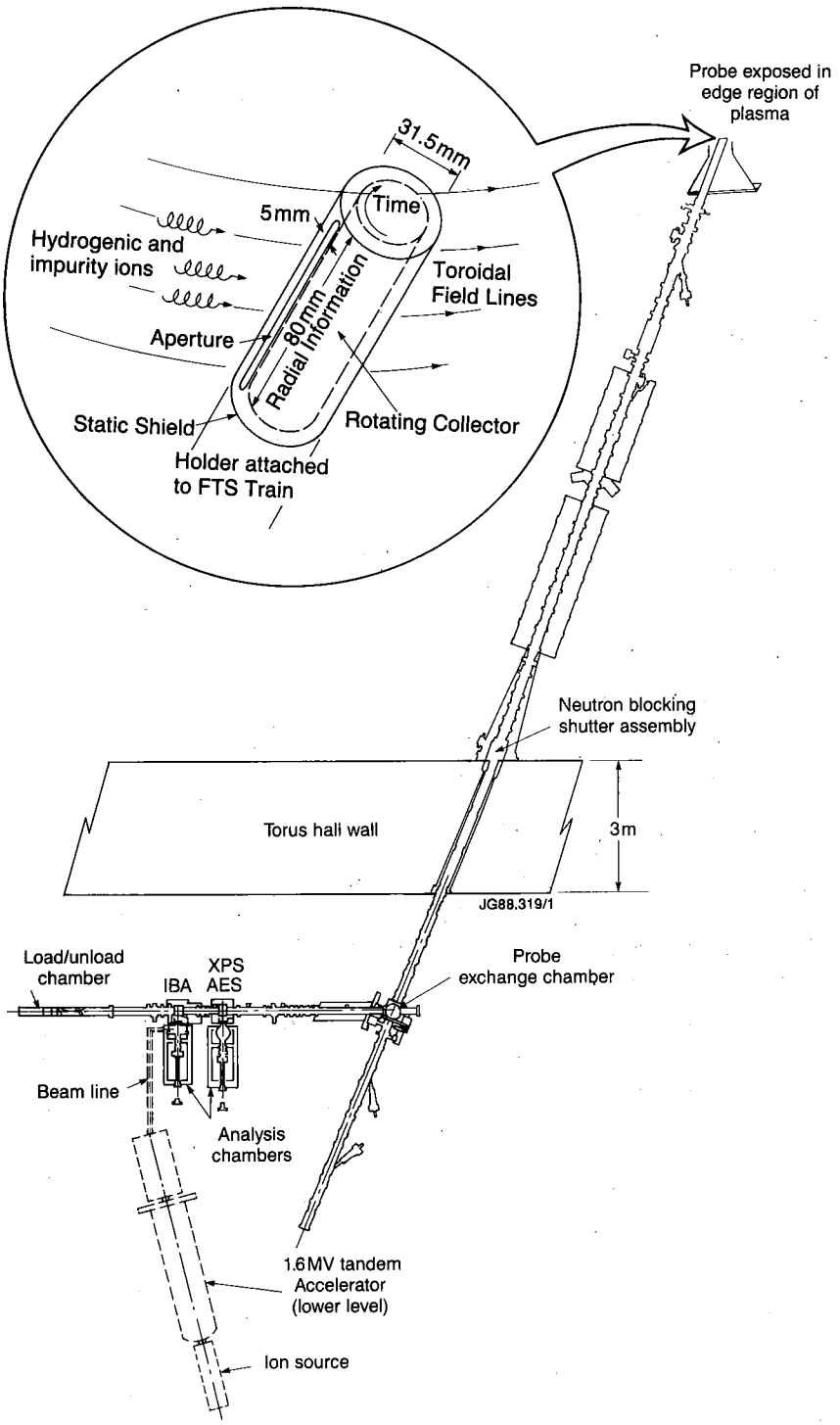

Fig. 2 Schematic view of the Fast Transfer System (FTS) and Surface Analysis System (SAS), with an inset showing a sketch of the collector probe and its orientation.

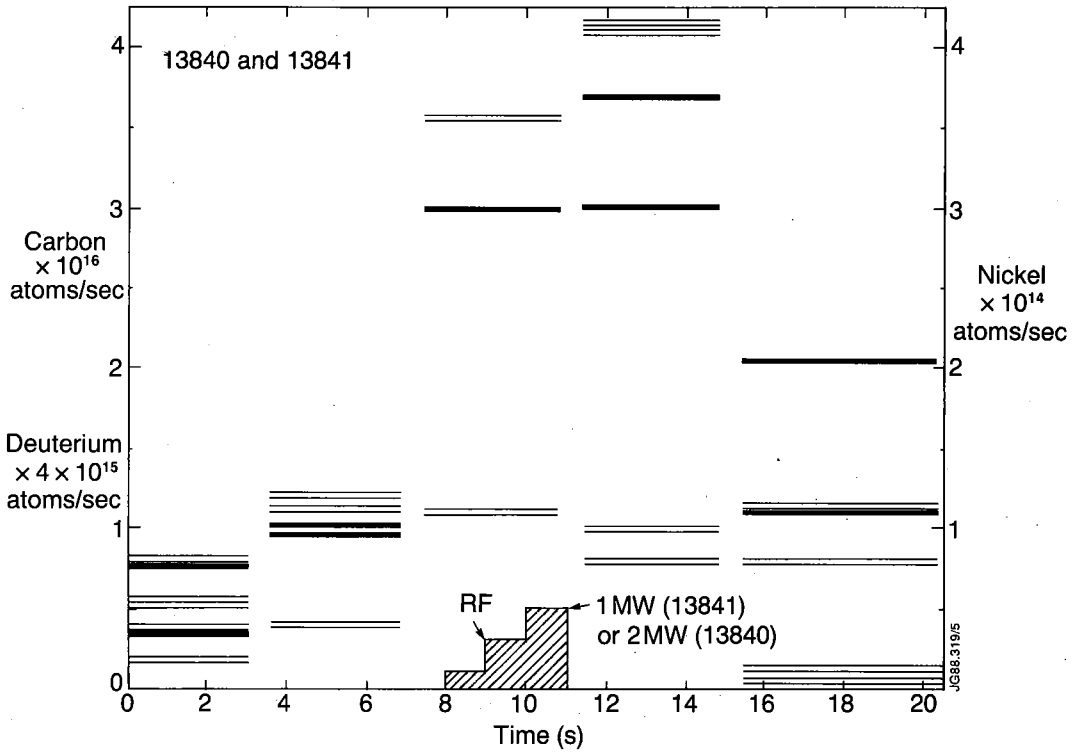

Fig. 3 The carbon, deuterium and nickel fluxes collected at a point 10 mm behind the RF antenna protection tiles for pulses 13840 and 13841.

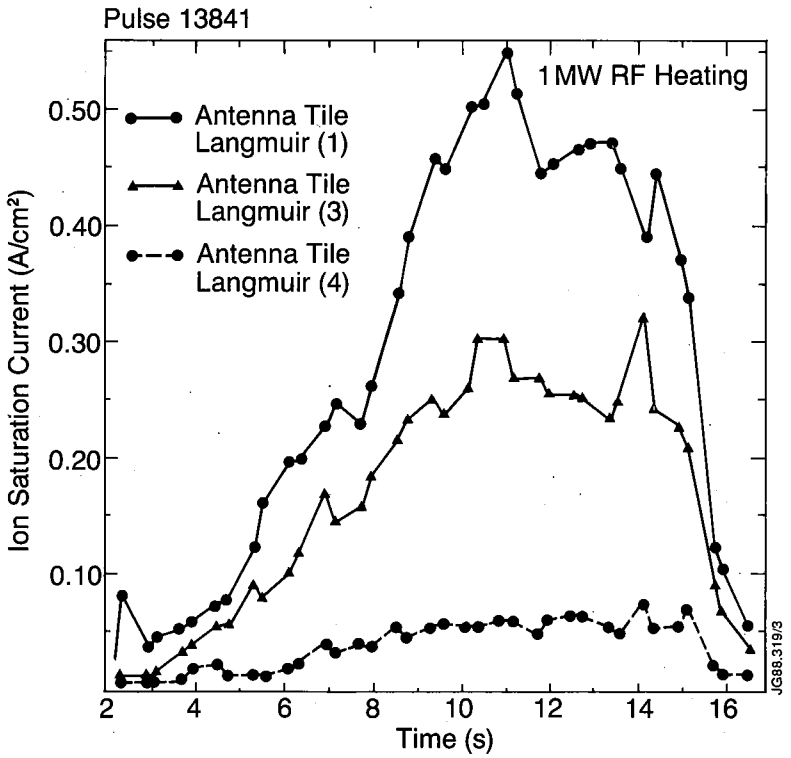

Fig. 4 The 'ion saturation current' measured with Langmuir probes at three points on RF antenna protection tiles for pulse 13841.

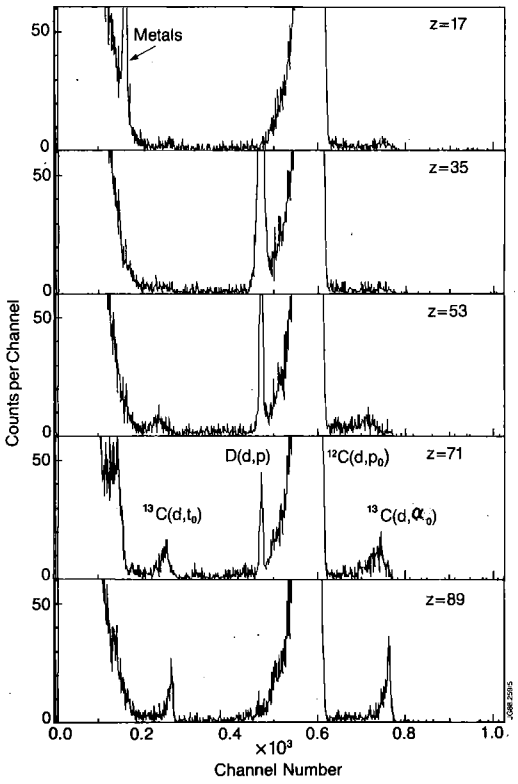

Fig. 5 Nuclear Reaction Analysis (NRA) spectra using a deuteron beam from five points along a collector probe exposed in the plasma boundary during the flat top of a 3 MA discharge (17928).

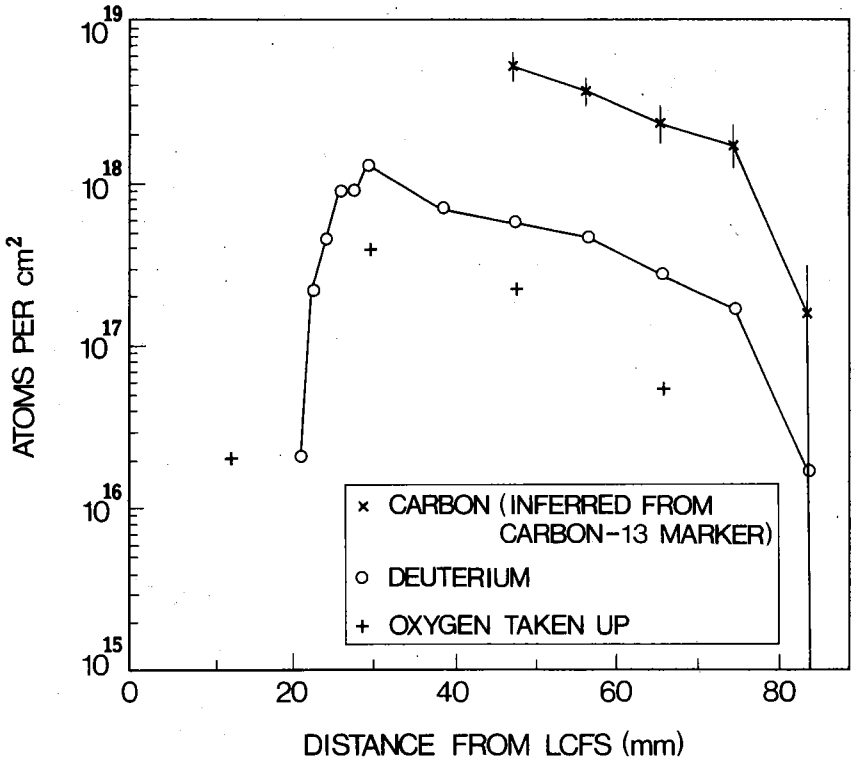

Fig. 6 The deuterium level observed along the probe exposed during the flat-top of pulse 17928, together with the amount of carbon inferred from the shift in the ^{13}C marker, and the amount of oxygen seen **after** exposure to air.

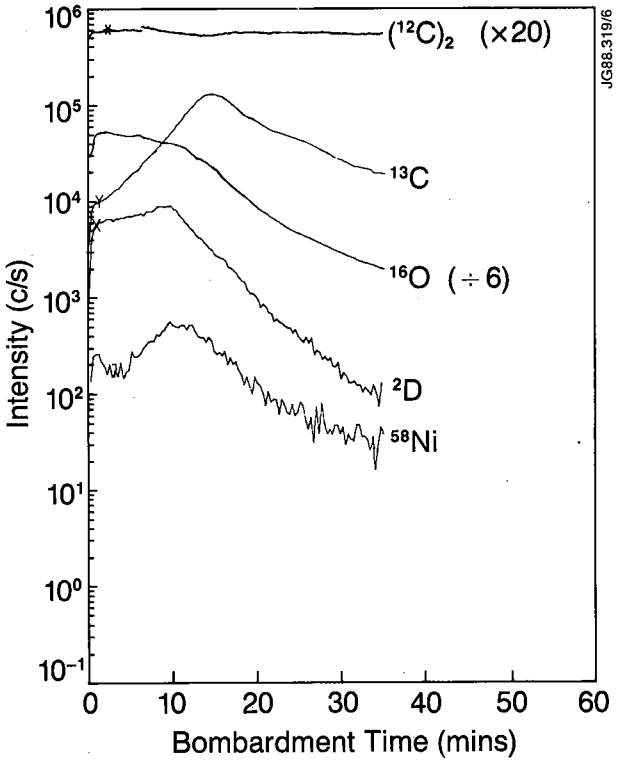

Fig. 7 SIMS analysis of carbon 12 (using mass 24), carbon 13, deuterium, oxygen and nickel from a point exposed ~70 mm from the LCFS during pulse 17928.

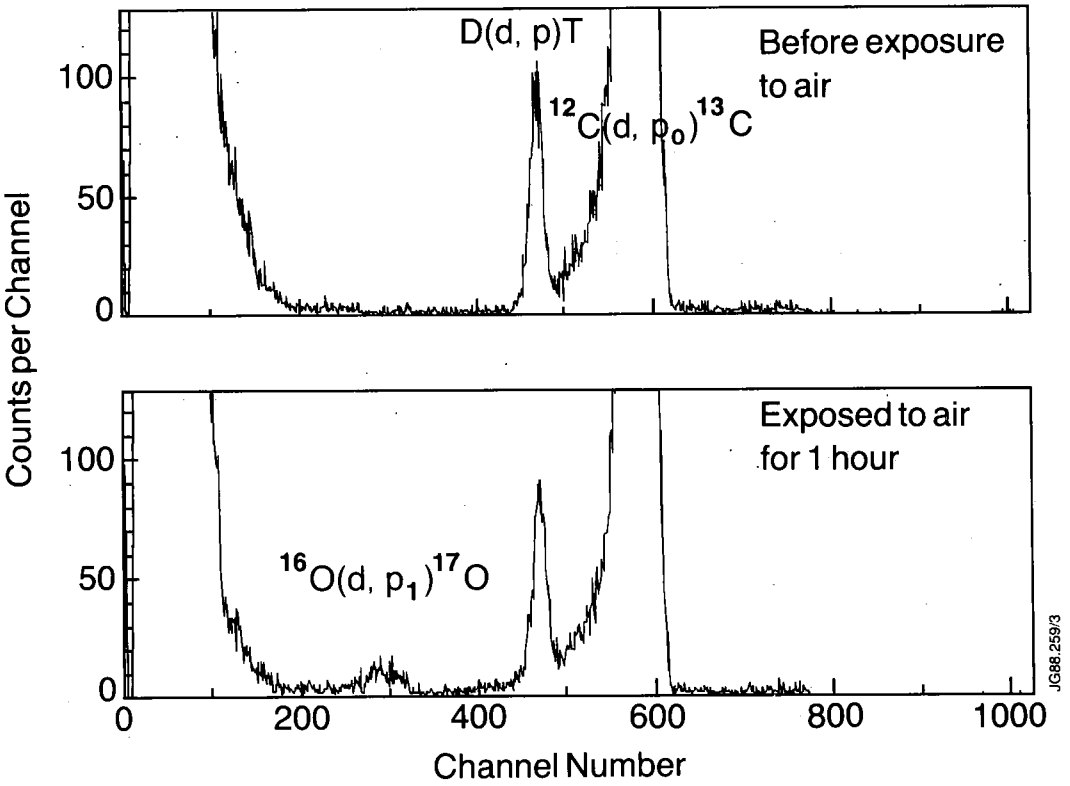

Fig. 8 NRA spectra recorded from the same point on an exposed carbon probe before and after exposure to air at atmospheric pressure for 1 hour.

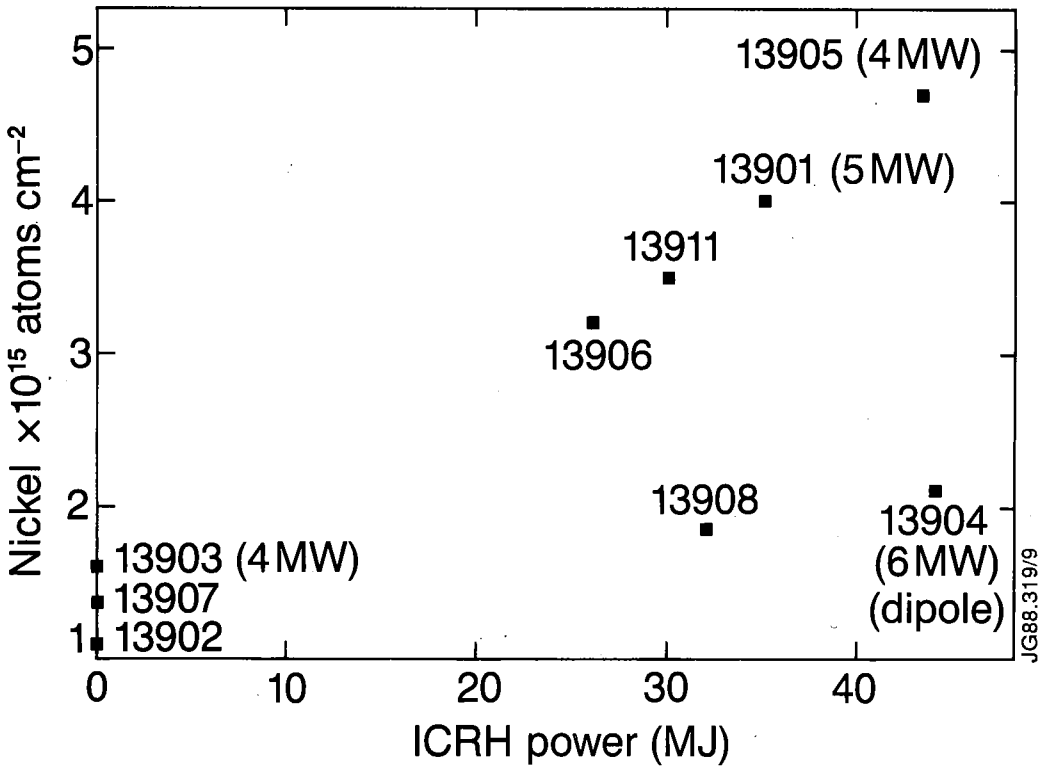

Fig. 9 The amount of nickel observed by PIXE exposed during 10 successive plasma pulses as a function of amount of RF heating power applied. The figures in brackets are the level of neutral beam heating power applied.

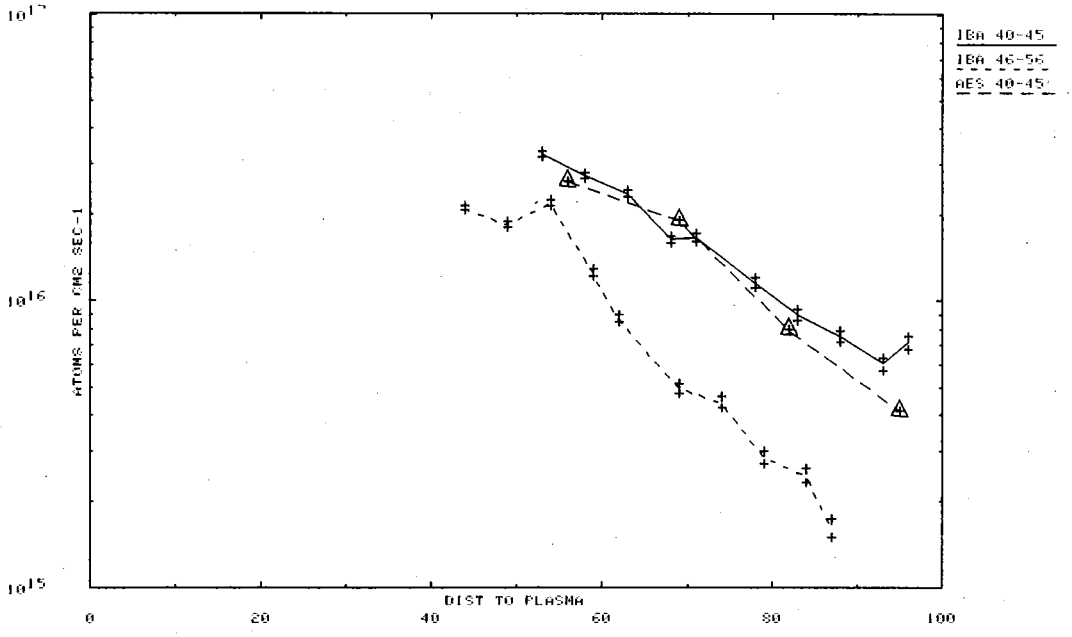

Fig. 10 A comparison of the amount of carbon derived from NRA and from Auger depth profiling as a function of distance along a collector probe (from the LCFS) exposed to the ramp-up of plasma current in pulse 18369, together with the NRA of the region exposed to the flat-top of the same pulse.